Suppression of chaos by resonant parametric perturbations

Ricardo Lima and Marco Pettini*
Centre de Physique Théorique, Luminy, Case 907, F-13288, Marseille CEDEX 09, France
(Received 9 August 1989)

Starting from a chaotic regime in the dynamics of a Duffing-Holmes oscillator, we show how it is possible, by means of a small parametric perturbation of suitable frequency, to bring the system to a regular regime. This situation is studied from the analytic point of view using the Melnikov method and from the numerical point of view computing Lyapunov exponents. The corresponding bounds for the perturbation are compared. Noting that the time, measured along the original unperturbed separatrix, that elapses between two successive homoclinic intersections grows when we approach the resonance, we propose a possible scenario for this type of regularization of the dynamics.

I. INTRODUCTION

The transition from regular to chaotic regime in nonlinear deterministic systems is by now well accepted; nevertheless, it still deserves a great deal of interesting work as it is not completely understood. At variance, here we deal with the opposite situation, namely, we show that a small but resonant parametric perturbation added to a system can change a chaotic regime into a regular one. This idea arises from the observation that parametric perturbations can change the stability properties of elliptic or hyperbolic points in the phase space of linear systems. In particular, a parametric resonant perturbation of the frequency of a linear oscillator at rest can excite it; on the contrary, a parametric forced oscillation of the pivot of a reversed pendulum can stabilize the usually unstable equilibrium position.[1] With these examples in mind, let us mention a heuristic (even if crude) reasoning that has suggested to us that parametric perturbations could also provide a mean to reduce or suppress chaos in nonlinear systems.

Let us remind that, if M is an n-dimensional smooth manifold, a "dynamical system"[2] is usually defined to be a one-parameter group of diffeomorphisms ϕ_t: $M \rightarrow M$ represented in local coordinates by $\dot{x}^i = f^i(x^1, \ldots, x^n)$. When the dynamical system is Hamiltonian, after Mapertuis's principle of least action, the trajectories are geodesics on the Riemannian manifold M equipped with the Jacobi metrics[3] $g_{ik}(x) = [h - U(x)]\delta_{ik}$. For nonautonomous Newtonian systems a different metric can be assigned to the enlarged configuration space including time.

Given a unit vector u tangent to M at a point x, $u \in T_1 M_x$, there is only one geodesic $\gamma(t)$ originating at x and having initial velocity u. A geodesic flow G_t on M is therefore defined as a one-parameter group of diffeomorphisms of the unitary tangent bundle $T_1 M$ sending $u(t_0) \in T_1 M_{\gamma(t_0)}$ to $u(t) \in T_1 M_{\gamma(t)}$, $(\dim T_1 M = 2n - 1)$.

The trajectories of a geodesic flow strongly depend on the stability properties of the geodesics on M; their stability can be studied by means of the Jacobi equation for the vector field of variations, which is obtained by a local linearization of the geodesic equation. Jacobi equation can be written[4] as

$$\frac{\nabla}{dt}\frac{\nabla}{dt}\xi(t) + \mathcal{R}_{\gamma(t)}(\xi(t), \dot{\gamma}(t))\dot{\gamma}(t) = 0 , \tag{1}$$

where ∇/dt is the covariant derivative, $\mathcal{R}$ is the curvature tensor, $\gamma(t)$ is the geodesic, and $\xi(t)$ is the Jacobi vector field.

Equation (1) describes the stability of nearby geodesics and $\xi(t)$ can be decomposed into parallel and perpendicular components to the vector $\dot{\gamma}(t)$. The Jacobi equation for the perpendicular component $\xi_\perp(t)$ can be cast in the form of a Newton equation[1]

$$\frac{\nabla}{dt}\frac{\nabla}{dt}\xi_\perp(t) = -\mathrm{grad}(R\langle \xi_\perp, \xi_\perp \rangle \langle \dot{\gamma}, \dot{\gamma} \rangle) , \tag{2}$$

where R is the Riemannian curvature in a section of the $(\xi_\perp, \dot{\gamma})$ plane. Now, for manifolds of constant curvature Eq. (2) gives $\ddot{\xi}_\perp + R\xi_\perp = 0$. If $R > 0$, the geodesics are stable, but for suitable $R = R(t)$ we could make them unstable by parametric resonance; loosely speaking, the regular solutions of a nonlinear integrable system (like a pendulum) could become chaotic by means of a parametric perturbation of such a system. This is, in fact, observed in systems like $\ddot{x} + [1 + \epsilon\cos(at)]\sin x = 0$. We remark that $R(t)$ in the Jacobi equation is, of course, related to the parametric perturbation of the equation of motion through the connection defined by the metric of configuration space. Anyway, we are oversimplifying things because we want to give just a heuristic argument. Then, to go on with our digression, we observe that when $R < 0$, as in the case of a Lobatchevsky plane, the geodesics are exponentially unstable, therefore the associated geodesic flow is stochastic. In this case, the Jacobi equation ends up precisely on the equation of motion of a reversed pendulum for which, as we said before, stabilization by parametric excitation is well known. This suggests that a stabilization of unstable geodesics could be attained by parametrically perturbing a chaotic system. In general, there is no reason to associate a geodesic flow on a manifold of constant negative curvature to a chaotic

dynamical system; if this were the case, after the Lobatchevsky-Hadamard theorem, it is known that such a geodesic flow should be a C flow and thus structurally stable, which is not the generic situation. Notice that within the previous analogy with the reversed pendulum, the scalar curvature in the Jacobi equation should "periodically change in time" as a consequence of a parametric perturbation of a given chaotic system in order to stabilize the geodesic flow.

Going on further with this analogy and making it more precise is beyond the aim of our present work and certainly is not a trivial task. In practice, to test these ideas, we have selected a nonlinear dynamical system whose chaotic transition can be controlled by some predictive analytical method, though approximate. Then we have been able to investigate, both analytically and numerically, the possibility of suppressing chaos by parametric perturbation.

We have chosen the Duffing-Holmes equation.[5] There are at least two types of reasons why we have chosen this model for our study. The first is that from the mathematical point of view, there is a sufficiently rich structure in the parameter space, where regions of well-developed chaos can be easily found and, under suitable conditions, analytical predictions can be made by means of the Melnikov method. The second is that, from the physical point of view, this equation was used to study plasma oscillations[6] which is the field of applications, even if remote, that we have in mind.

We have found that, as expected from the previous arguments, starting from a chaotic regime, a regular motion is recovered only for some values of the perturbation frequency, while perturbations of near resonant frequencies still reduce the Lyapunov exponent. Finally, we want to remark that in many real physical systems (like tokamaks,[7] particle accelerators,[8] etc.), chaotic regimes can have harmful consequences and one would dream to find effective mechanisms to reduce or eliminate the chaotic instability of the dynamics without radically changing the hardware of a given system.

II. SYSTEM

As mentioned before, we study the Duffing-Holmes equation with a parametric perturbation of the cubic term

$$\ddot{x}-x+\beta[1+\eta\cos(\Omega t)]x^3=-\delta\dot{x}+\gamma\cos(\omega t)\ , \tag{3}$$

where η is the amplitude and Ω the frequency of the parametric perturbation. Here it should be $\eta \ll 1$.

For $\eta=0$ we recover the usual Duffing-Holmes oscillator; the parameters δ and γ are assumed small and proportional to some smallness parameter, so that the right-hand side (rhs) of Eq. (3) is a nonautonomous and dissipative perturbation of a system described by the following Hamiltonian:

$$H(p,x)=\tfrac{1}{2}(p^2-x^2+\tfrac{1}{2}\beta x^4)\ . \tag{4}$$

From the general theory of hyperbolic points applied to the saddle point (0,0), one knows of the existence of stable W^s and unstable W^u manifolds which, in this case, form a homoclinic loop. In the presence of dissipation, the homoclinic loop is destroyed and W^u and W^s never meet. Nevertheless, a homoclinic intersection point can be recovered by adding a forcing, provided that its amplitude exceeds a critical value. This is a well-known situation where chaos may arrive.[9] Furthermore, in the present case a criterion, due to Melnikov,[10] for the existence of chaotic motion applies.

The method consists in evaluating the distance $\Delta(t_0)$ between W^u and W^s at time t_0, measured along the homoclinic loop, and checking if $\Delta(t_0)$ changes sign for some t_0. The computation is performed up to first-order perturbation theory.

Following Ref. 9, the Melnikov distance for the Duffing-Holmes oscillator is given by

$$\Delta_0(t_0)=2\pi\left[\frac{2}{\beta}\right]^{1/2}\gamma\omega\,\mathrm{sech}\left[\frac{\pi\omega}{2}\right]\sin(\omega t_0)+\frac{4\delta}{3\beta}\ . \tag{5}$$

We compute, along the same line, the corresponding quantity for Eq. (3). First, notice that, corresponding to the hyperbolic fixed point of (4), the homoclinic loop is given by

$$\begin{aligned} x_0(t)&=\left[\frac{2}{\beta}\right]^{1/2}\mathrm{sech}t\ , \\ p_0(t)&=-\left[\frac{2}{\beta}\right]^{1/2}\mathrm{sech}t\tanh t\ . \end{aligned} \tag{6}$$

Therefore, in presence of parametric perturbation, we get (see the Appendix)

$$\Delta(t_0)=\Delta_0(t_0)-\frac{\eta}{\beta}\int_{-\infty}^{\infty}dt\,p_0(t-t_0)\times[x_0(t-t_0)]^3\cos(\Omega t)\ . \tag{7}$$

Denoting by D_η the integral in the right-hand side of (7), we write

$$\begin{aligned} D_\eta&=\frac{4\eta}{\beta}\int_{-\infty}^{\infty}dt\,\mathrm{sech}^4(t-t_0)\tanh(t-t_0)\cos(\Omega t) \\ &=\frac{4\eta}{\beta}\sin(\Omega t_0)\int_{-\infty}^{\infty}d\tau\,\mathrm{sech}^4\tau\tanh\tau\sin(\Omega\tau) \\ &=\frac{4\eta}{\beta}\sin(\Omega t_0)\int_{-\infty}^{\infty}d\tau\cosh^{-5}\tau\sinh\tau\sin(\Omega\tau)\ . \end{aligned} \tag{8}$$

The last integral can be performed by the method of residues to yield

$$\int_{-\infty}^{\infty}d\tau\cosh^{-5}\tau\sinh\tau\sin(\Omega\tau)=\frac{\pi}{24}(\Omega^4-6\Omega^2+1)\mathrm{csch}\left[\frac{\pi\Omega}{2}\right]\ . \tag{9}$$

Therefore we get

$$D_\eta=\frac{\pi\eta}{6\beta}(\Omega^4-6\Omega^2+1)\mathrm{csch}\left[\frac{\pi\Omega}{2}\right]\sin(\Omega t_0)\ , \tag{10}$$

and gluing together (5), (7), and (10), we finally obtain

$$\Delta(t_0)=\frac{2\sqrt{2}}{\sqrt{\beta}}\pi\gamma\omega\,\mathrm{sech}\left[\frac{\pi\omega}{2}\right]\sin(\omega t_0)+\frac{4\delta}{3\beta}+\frac{\pi\eta}{6\beta}(\Omega^4-6\Omega^2+1)\mathrm{csch}\left[\frac{\pi\Omega}{2}\right]\sin(\Omega t_0)\ . \quad (11)$$

With obvious notation, we rewrite Eq. (11) in the following form:

$$\Delta(t_0)=A(\omega)\sin(\omega t_0)+B(\Omega)\sin(\Omega t_0)+C\ . \quad (12)$$

For a better understanding of the discussion below, we have plotted $A(\omega)$ and $B(\Omega)$ in Fig. 1.

Let us first consider the effect of the modulus of the correction $B(\Omega)$, disregarding the phase factors initially set equal to 1. Suppose that we are in a chaotic situation for which the original Melnikov distance Δ_0 changes sign at some t_0, i.e.,

$$A(\omega)-C=d>0\ . \quad (13)$$

Then, as it is clear from (12), if

$$|B(\Omega)|<d\ , \quad (14)$$

the situation remains unchanged, i.e., for some t_0, Δ will change sign. This is, in particular, the case if the frequency Ω is such that $B(\Omega)\geq 0$, i.e., $\Omega<0.414$ or $\Omega>2.414$ (see Fig. 1).

A necessary condition for Δ to be positive for all t_0 is then $B(\Omega)<-d$ or, equivalently,

$$\eta>\left|\frac{6\beta d}{\pi(\Omega^4-6\Omega^2+1)\mathrm{csch}(\pi\Omega/2)}\right|\ . \quad (15)$$

But, for a general Ω, we shall see that this condition is not sufficient to assure the positivity of Δ. It turns out, as it is shown in the following lemma, that condition (15) is sufficient if the frequency Ω is in resonance with the driving frequency ω.

Lemma 1. Let $p\Omega=q\omega$ for some integers p and q, then $\Delta(t_0)$ always has the same sign, i.e., $\Delta(t_0)>0$, if and only if condition (15) is fulfilled.

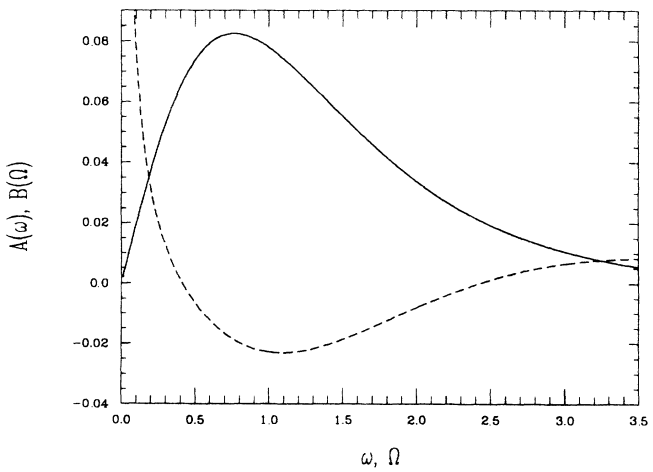

FIG. 1. Functions $A(\omega)$ and $B(\Omega)$ in Eq. (12) are computed here for $\beta=4$, $\delta=0.154$, $\gamma=0.088$, $\omega=1.1$, and $\eta=0.1$. Solid line represents $A(\omega)$ and dashed line $B(\Omega)$.

Proof. We have

$$\Delta(t_0)=A(\omega)\sin(\omega t_0)+B(\Omega)\sin(\Omega t_0)+C\geq-[A(\omega)+B(\Omega)]+C\ , \quad (16)$$

and therefore condition (15) implies $\Delta(t_0)>0$. The converse follows from the existence of a value of t_0 such that

$$\sin(\omega t_0)=\sin(\Omega t_0)=-1\ . \quad (17)$$

This is a consequence of the resonance condition.

Remark. If the second term on the rhs of Eq. (12) is replaced by $\sin(\Omega t_0+\varphi)$, with φ in a small range of values, the above reasoning breaks. However, our numerical simulations showed that the result concerning suppression of chaos is phase independent. See also the remark after Lemma 2.

We now turn to the nonresonant case, for which we prove the following.

Lemma 2. Let Ω/ω be irrational and let η fulfill condition (15). Then there is some t for which $\Delta(t_0)$ changes sign.

Proof. As mentioned before, the result is trivial if (14) is verified. If not, let t_0 be such that

$$\Delta_0(t_0)=A(\omega)\sin(\omega t_0)+C<0\ . \quad (18)$$

By (15), there is then $\epsilon>0$ such that

$$[A(\omega)-B(\Omega)]\epsilon<\Delta(t_0)\ . \quad (19)$$

Because Ω/ω is irrational, a well-known argument[11] shows the existence of a t fulfilling simultaneously the following two inequalities:

$$|\sin(\Omega t)|<\epsilon \quad (20)$$

and

$$|\sin(\omega t)-\sin(\omega t_0)|<\epsilon\ , \quad (21)$$

and therefore the Lemma follows.

Remark. In the case where Ω is close to a resonance, we estimate the time T elapsed between two changes of sign of the Melnikov function.

In order to do this, we first notice that condition (20) is equivalent to

$$|\Omega T-k\pi|<\arcsin\epsilon \quad (22)$$

for some integer k, or

$$\left|T-\frac{k\pi}{\Omega}\right|<\frac{1}{\Omega}\arcsin\epsilon\ . \quad (23)$$

And since

$$\left|\sin(\omega T)-\sin(\omega t_0)\right|=2\left|\cos\left[\omega\frac{T+t_0}{2}\right]\sin\left[\omega\frac{T-t_0}{2}\right]\right|\leq 2\left|\sin\left[\omega\frac{T-t_0}{2}\right]\right|\ , \quad (24)$$

we get the following sufficient condition for (21)

$$|\omega T-\omega t_0-4\pi l|\leq 2\arcsin\frac{\epsilon}{2} \tag{25}$$

or

$$|T-t_0-\frac{4\pi l}{\omega}|\leq\frac{2}{\omega}\arcsin\frac{\epsilon}{2}\ . \tag{26}$$

Condition (23), together with (26), simply means that T is a point in the intersection of two intervals of the real line. Let $\bar{\epsilon}$ be a constant (of the order of ϵ) which is the maximum of the right-hand sides of (22) and (25). Then the existence of such a T is equivalent to the following condition:

$$\left|t_0+\frac{2\pi l}{\omega}-\frac{k\pi}{\Omega}\right|<\bar{\epsilon}\left[\frac{1}{\omega}+\frac{1}{\Omega}\right]\ . \tag{27}$$

Let us now take, for simplicity, the case of the principal resonance $\Omega\simeq\omega$, since the other resonant cases can be treated in the same way. Denote

$$\alpha=\left\{\frac{\omega}{\Omega}\right\} \tag{28}$$

and

$$\beta=\left\{\frac{t_0\omega}{\pi}\right\}\ , \tag{29}$$

where the curly brackets stand for the fractionary part of a real number.

Then (27) can be written, changing the integers k and l, in the following form:

$$|\beta+l-k\alpha|<\frac{\delta}{\pi}\ , \tag{30}$$

where δ (again of order ϵ) is such that

$$\bar{\epsilon}(\omega+\Omega)\leq 2\delta\Omega\ . \tag{31}$$

Now, in our case α can be taken smaller than δ/π and therefore, uniformly in β, k is near $1/\alpha$.

Because Ω is near the principal resonance we have

$$\alpha=\left\{\frac{\omega}{\Omega}\right\}=\left|1-\frac{\omega}{\Omega}\right|=\frac{|\Omega-\omega|}{\Omega}\ , \tag{32}$$

and therefore

$$T\sim\frac{k\pi}{\Omega}=\frac{\pi}{|\Omega-\omega|}\ . \tag{33}$$

To be more precise, we notice that this estimate is obtained in the limit $A(\omega)-B(\Omega)-C=\rho\simeq 0$, i.e., when a condition of homoclinic tangency is approached.

Now, let $B(\Omega)$ vary through Ω or η. From Eq. (12) it can be seen that critical values exist for ρ such that, when it is increased, new intermediate intersection times suddenly appear. These times are near the submultiples of T (the quasiperiod). These successive bifurcations of the first intersection time [given by the first simple zero of $\Delta(t_0)$] are responsible for the observed jumps of the function $\tau_M^{-1}(\Omega)$ reported in Figs. 2 and 3.

When η is increased, ρ decreases. This yields a lowering of the number n of intermediate times and therefore one can roughly estimate the time τ_M^{-1} of the first homoclinic intersection to be T/n.

The scaling of T given by (33), and therefore that of τ_M^{-1}, is actually observed near the resonance (see Figs. 2 and 3). We notice that this estimation is phase independent, and since it shows that the time elapsed between two successive changes of sign in the Melnikov function tends to infinity as resonance is approached, it provides an analytic explanation for the observed suppression of chaos.

In Figs. 2 and 3 the function $\tau_M^{-1}(\Omega)$ is reported for a large interval of values of Ω. Let us just mention that the low-frequency feature of this function is a consequence of the beating of the two oscillating terms in Eq. (12) when $A(\omega)\simeq B(\Omega)$.

Moreover, a striking analogy appears between the behavior of $\tau_M^{-1}(\Omega)$ and the behavior of the Lyapunov exponent $\lambda(\Omega)$ (near the principal resonance), which is shown in Sec. III. This suggests the existence of a deeper relation between the two quantities. Thus we guess that a variation of Ω near a resonance entails a scaling of the dynamics given by that of τ_M. The fact that the estimation of τ_M is performed in the neighborhood of the reference homoclinic point confirms the importance of this region of phase space with respect to global chaotic behavior.[12] This is to say that, when Ω varies, a given divergence of nearby orbits is attained in a time which scales as τ_M. Furthermore, this guess is supported by the same qualitative dependence of $\lambda(\Omega)$ and $\tau_M^{-1}(\Omega)$ on the parameter η; according to the above remark, this behavior is related to the change of the number n as a function of η. Indeed, it can be seen in Figs. 2 and 3 that, keeping Ω fixed, τ_M^{-1} decreases when η increases. The previous considerations can be rephrased as follows:

$$\lambda\sim\frac{|\Omega-\omega|}{n}\ln\Lambda(\Omega,\eta)\ . \tag{34}$$

The second factor on the rhs is likely to give only a logarithmic correction when Ω or η vary, the reason being that the ratio of the two natural lengths in our problem,

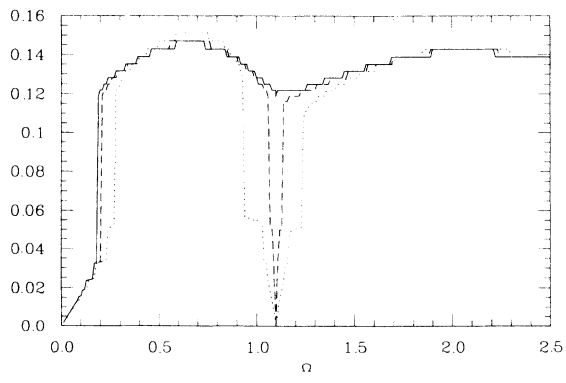

FIG. 2. The inverse of the time τ_M elapsed between two successive homoclinic intersections, computed using Eq. (11), is plotted vs the parametric perturbation frequency Ω. Again $\beta=4$, $\delta=0.154$, $\gamma=0.088$, and $\omega=1.1$. The solid line corresponds to $\eta=0.09$, dashed line to $\eta=0.1$, and dotted line to $\eta=0.15$.

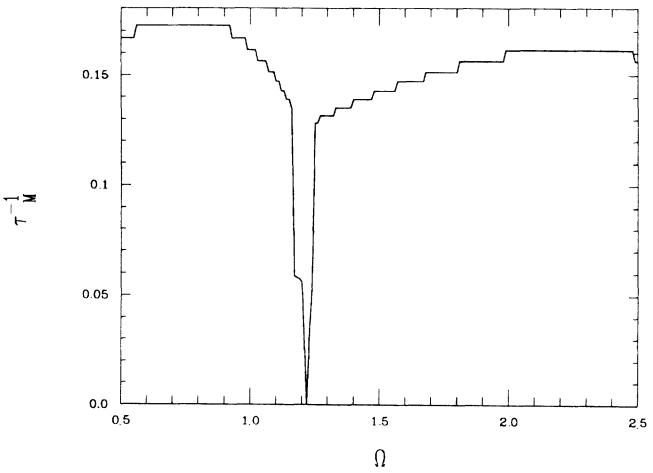

FIG. 3. τ_M^{-1} vs Ω is reported for $\beta=4$, $\delta=0.154$, $\gamma=0.114$, $\omega=1.22$, and $\eta=0.17$.

which appear in $\Lambda(\Omega,\eta)$, may vary slowly with the parameters (Ω,η). In fact, they are related to the iterates of points close to each other that tend to approach the attractor along or close to the unstable manifold W^u, crossing between left and right half-planes in an erratic way (see Ref. 13). Hence we are led to think that $\Lambda(\Omega,\eta)$ scales as the distance of the two sinks of the initial system divided by ρ. Therefore the factor $\ln\Lambda(\Omega,\eta)$ only introduces a small correction in the above reported scaling of λ.

III. NUMERICAL RESULTS

We have performed some computer simulations on the system described by Eq. (3). We have mostly adopted a fourth-order Hammings modified predictor-corrector. Some comparisons have also been carried on by means of fourth-order Runge-Kutta method to rule out possible algorithm-dependent effects.

Not only a systematic numerical survey of the parameter space of Eq. (3) is beyond our aims, but this would be prohibitive because of its high dimension. Therefore we have chosen some arbitrary sets of parameters, for the unperturbed part of Eq. (3), such that the Melnikov criterion was largely satisfied; then we verified also numerically that chaos was actually present after having eliminated a long transient. In choosing our sets of parameters, we took advantage of an existing numerical study of a subset of parameter space[14] of Eq. (3) at $\eta=0$. Regular and chaotic motions were detected by usual methods: Lyapunov characteristic exponent, power spectrum, and correlation function of the solution.

The Lyapunov exponent λ is the most practical chaoticity indicator for our purposes. Equation (3), cast in the form of a first-order system

$$\dot{\mathbf{x}}=\mathbf{F}(\mathbf{x},t)\ , \tag{35}$$

is numerically integrated together with the dynamics in tangent space described by

$$\dot{w}_i=\sum_j \left[\frac{\partial F_i}{\partial x_j}\right]_{\mathbf{x}(t)} w_j\ , \tag{36}$$

where the Jacobian matrix $(\partial F_i/\partial x_j)$ is computed along the trajectory $\mathbf{x}(t)$.

The Lyapunov exponent is then given by

$$\lambda=\lim_{t\to\infty}\frac{1}{t}\ln\frac{\|\mathbf{w}(t)\|}{\|\mathbf{w}(0)\|}\ . \tag{37}$$

A standard reprojection technique[15] has been adopted for numerical evaluation of (37).

Numerical experiments have been performed on a CRAY X-MP 48 computer. Time steps have been chosen in the range $\Delta t=0.001,0.003$ to make the algorithm error [which is of order $(\Delta t)^5$] of the same order of magnitude of the computer round-off error. Typically, Eqs. (35) and (36) have been integrated up to $t=15\,000$.

In Fig. 4, λ versus Ω is reported. The equation of motion has been integrated at fixed parametric perturbation amplitude $\eta=0.03$. The dotted line corresponds to the unperturbed value of λ obtained at $\eta=0$. Figure 4 is composed of two different sets of points: the first is a coarse-grained scanning of the interval $\Omega\in[0.15,3.8]$ with $\Delta\Omega=0.1$, the second is a denser collection of points around multiples and submultiples of the forcing frequency ω (after Lemma 1 these are the relevant regions to investigate).

The striking result is that for $\Omega\simeq\Omega_R^{(k)}\equiv k\Omega_R^{(1)}$ the Lyapunov exponent vanishes and thus a regular motion is actually recovered. The $\Omega_R^{(k)}$ are the harmonics of the forcing frequency ω, hence the parametric resonance "spectroscopy" is rather simple.

We found also that λ can vanish for $\Omega=\frac{1}{2}\Omega_R^{(1)}$, $\frac{3}{2}\Omega_R^{(1)}$, and $\frac{5}{2}\Omega_R^{(1)}$, and it can be lowered only in very narrow regions around the resonant values, i.e., when the resonance mismatch is $|\delta\Omega|<0.002$. But these subharmonic resonances have a sensitive dependence on the starting point in phase space, so that both regular and chaotic solutions can be found. The values of $\lambda(\Omega)$, computed off-resonance with $\eta\neq0$, are close to the unperturbed $(\eta=0)$ value of λ.

It is worth mentioning that the convergence of λ is fast and the residual fluctuations are very small in the follow-

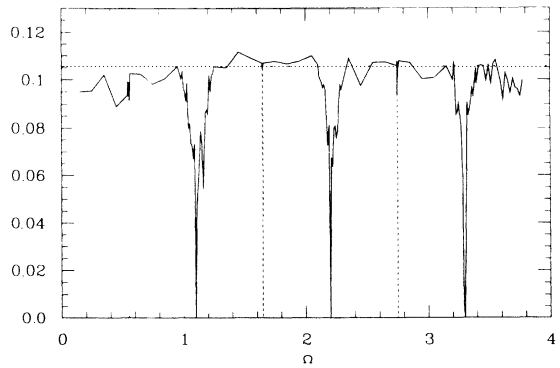

FIG. 4. The maximum Lyapunov characteristic exponent λ is reported vs Ω. This result corresponds to $\beta=4$, $\delta=0.154$, $\gamma=0.088$, $\omega=1.1$, and $\eta=0.03$. The dotted line refers to $\eta=0$ (unperturbed case) for which $\lambda=0.1056$. Dotted lines are also used for subharmonic resonances whose existence depend on the starting point in phase space.

ing cases: (i) $\eta=0$, (ii) $\eta\neq 0$ and Ω off-resonance, and (iii) $\eta\neq 0$ and $\Omega=\Omega_R^{(k)}$. At variance, when Ω is nearly resonant the convergence of λ is slowed down and persistent fluctuations show up of typical magnitude $\Delta\lambda/\lambda=0.01-0.02$ around some average value. These fluctuations do not seem to be due to a numerical artifact because they do not change when the reprojection time interval is varied, the integration time step is reduced, or the overall integration time is increased.

Finally, notice that we observed $\lambda(\Omega_R^{(k)})=0$ for $k=1,2,3$, while for higher k the perturbation does not even lower λ.

Not only the theoretical prediction of suppression of chaos for $\Omega=\Omega_R^{(1)}$ is verified, but also a resemblance between $\tau_M^{-1}(\Omega)$ and $\lambda(\Omega)$ is observed near $\Omega_R^{(1)}$ (see also Fig. 5).

On the other side, the analytical prediction in Eq. (15) overestimates the threshold for η; Fig. 2 shows that, for a given set of parameters of the unperturbed system, $\eta=0.09$ is not sufficient to suppress chaos while numerical simulations already give $\lambda(\Omega_R^{(1)})=0$ with $\eta=0.01$. Another thing that is not theoretically explained is the existence of higher resonances, i.e., $\lambda(\Omega_R^{(2)})=0$ and $\lambda(\Omega_R^{(3)})=0$. But these problems are not surprising because Melnikov's method, being based on perturbation theory, is approximate.

In Fig. 5 a more detailed structure of λ versus Ω is given in the neighborhood of $\Omega_R^{(1)}$. In Fig. 6 the same detail is given for different values of the perturbation amplitude η; a "line broadening" is observed when η is increased. This is in good qualitative agreement with the behavior of $\tau_M^{-1}(\Omega)$ reported in Fig. 2. In Fig. 7 the principal resonance is reported for a different set of the unperturbed system just to provide an example of the generic character of the results.

Another way of detecting the same phenomenon is by looking at the spectral properties of the solutions. From numerical integration one obtains pseudo-orbits of the system in the form of time series $\{x(t_0),x(t_1),\ldots,x(t_m)\}$, then standard fast Fourier transform yields the power spectrum $S(\omega_n)=|\tilde{x}(\omega_n)|^2$, where $\omega_n=2\pi n/m\Delta T$ and $\Delta T=t_k-t_{k-1}$ is the sampling time. Usual averaging procedures have been used to improve its quality.

In Fig. 8 we show how $S(\omega_n)$ is modified approaching a resonant value of Ω. Comparison among Figs. 8(a)–8(c) clearly shows that when $\Omega\rightarrow\Omega_R^{(1)}$, the random component of the spectrum is reduced and its periodic component is magnified. By Fourier transforming $S(\omega_n)=|\tilde{x}(\omega_n)|^2$ after setting $S(0)=0$, the normalized autocorrelation function $C(\tau_i)=\langle x(t)x(t+\tau_i)\rangle_t/\langle x^2(t)\rangle_t$, with $\tau_i=i\Delta T$, has been finally computed for different values of Ω.

When Ω is far from any $\Omega_R^{(k)}$, $C(\tau_i)$ is damped, which is typical of chaotic motion where memory loss of initial conditions is present. If Ω gets closer to some resonant

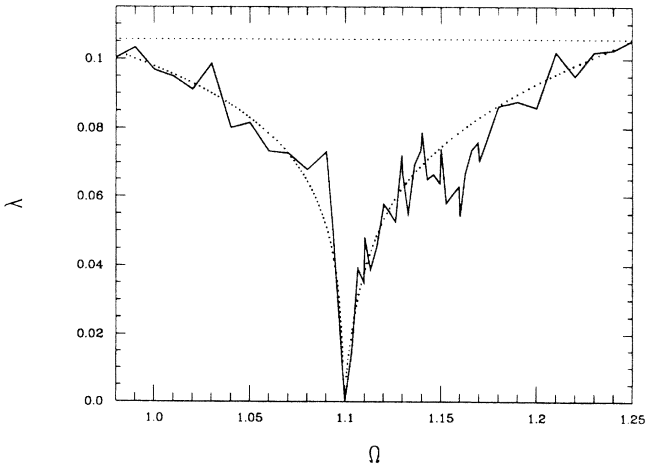

FIG. 5. Detail of λ vs Ω near the principal resonance. The parameters are $\beta=4$, $\delta=0.154$, $\gamma=0.088$, $\omega=1.1$, and $\eta=0.03$. Dotted line is a free-hand smoothing given as an eye guide.

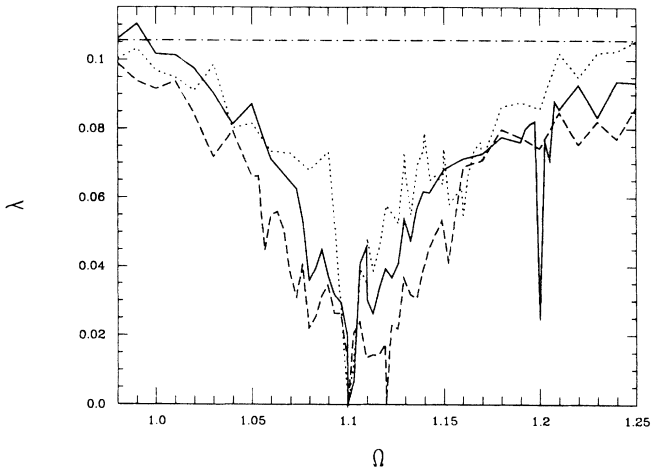

FIG. 6. λ vs Ω for $\beta=4$, $\delta=0.154$, $\gamma=0.088$, and $\omega=1.1$ at different parametric perturbation amplitude. The dotted line corresponds to $\eta=0.03$, solid line to $\eta=0.05$, and dashed line to $\eta=0.07$.

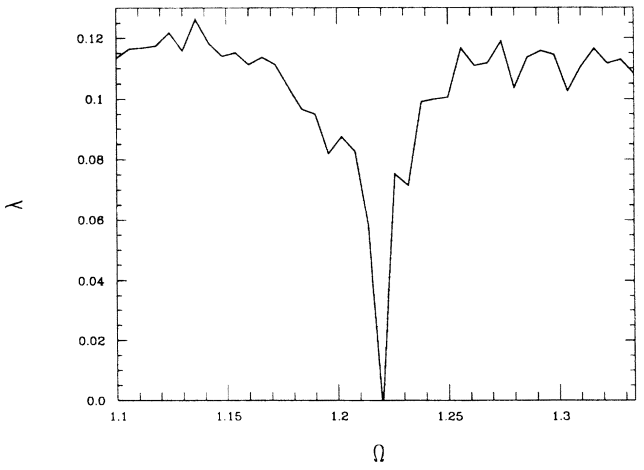

FIG. 7. λ vs Ω near the principal resonance for a different set of parameters $\beta=4$, $\delta=0.154$, $\gamma=0.114$, $\omega=1.22$, and $\eta=0.04$.

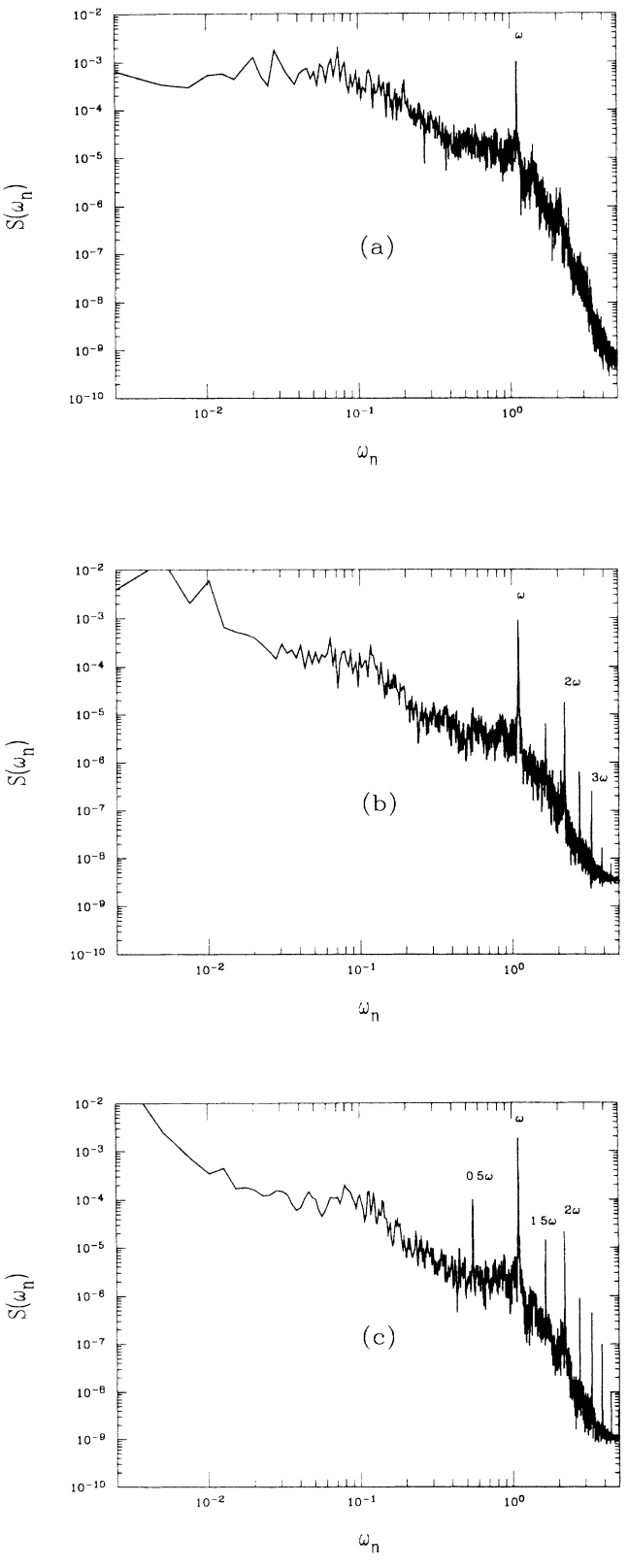

FIG. 8. Power spectrum $S(\omega_n)=|\bar{x}(\omega_n)|^2$ of the solution of Eq. (3) for $\beta=4$, $\delta=0.154$, $\gamma=0.088$, $\omega=1.1$, and $\eta=0.03$; (a) $\Omega=1.3$, (b) $\Omega=1.103$, and (c) $\Omega=1.101$. These are obtained by averaging over 10 meshes of 2^{13} points with a sampling time $\Delta T=0.6$. Time integration step is $\Delta t=0.002$.

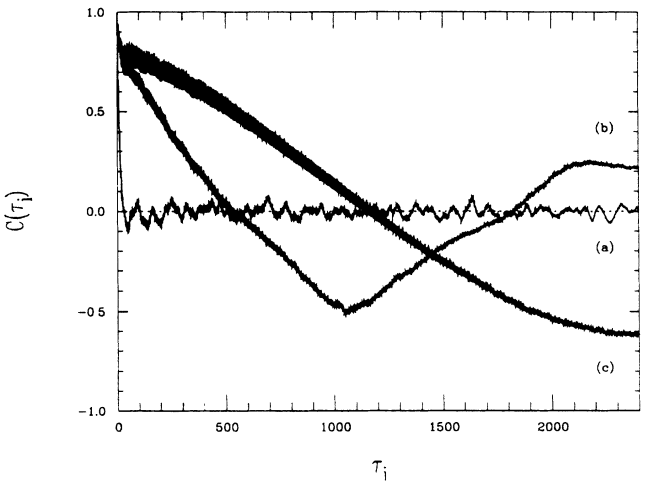

FIG. 9. Autocorrelation function $C(\tau_i)$ obtained by Fourier transforming the spectra of Fig. 8. Curves (a), (b), and (c) correspond to the homonymous cases of Fig. 8. The thickness of the curves (b) and (c) is due to graphical squeezing of oscillations at frequency ω.

value, then $C(\tau_i)$ displays a slower damping, which means that the time scale of memory loss gets larger, in qualitative agreement with the decrease of Lyapunov exponent.

In Fig. 9 three different cases are provided: an off-resonance example yielding a quickly damped $C(\tau_i)$ almost identical to the unperturbed case at $\eta=0$, and two nearly resonant examples where $C(\tau_i)$ displays oscillations of very long period and slowly damped. When $\Omega=\Omega_R^{(k)}$, we find that $C(\tau_i)$ is an undamped sinusoid, this means that $\mathbf{x}(t)$ has been attracted by a periodic solution, which, in particular, is a period-one solution. Analogous results were obtained for different sets of parameters of the unperturbed system. Finally, it is worth mentioning that all the observed phenomenology is independent of the initial phase shift between the two cosines in Eq. (3).

IV. CONCLUSIONS

In this article we considered the effect of a small parametric perturbation on the Duffing-Holmes equation (3), i.e., we have introduced a small and periodic oscillation of the coefficient in the cubic term of that equation. We start from a nonperturbed situation ($\eta=0$) in which the solutions of the equation approach a limiting set which looks like a strange attractor (see Ref. 13). In this nonperturbed case the system has a positive Lyapunov exponent, thus the dynamics is chaotic.

The addition of a parametric perturbation turned out to be able to make regular this chaotic dynamics. The dynamics becomes regular provided that the perturbation amplitude is larger than some critical value (for the standard set of parameters used, it is $\simeq 0.01$ of the corresponding unperturbed term) and that the frequency is in resonance with that of the forcing term (an effect up to the third harmonic was present).

This fact was confirmed either by an analytic estimation or by numerical computations. The Melnikov

method has proved useful to predict the possibility of regularizing chaotic dynamics and to estimate the threshold of this regularization transition. As this is a first-order perturbative method, the quantitative predictions are not accurate. Nevertheless, the estimates of the homoclinic intersection times and of the oscillation amplitudes of the stable and unstable manifolds give interesting indications about the behavior of the Lyapunov exponent λ near the principal resonance. In particular, it gives information about the scaling and the direction of variation of λ as function of the perturbation parameters. Numerical computations of λ confirmed the possibility of suppressing chaos (λ becomes zero). This phenomenon occurs for values of the perturbation amplitude greater than $\simeq 0.1$ times the theoretically estimated value and for a range of resonant frequencies larger than expected. This seems to indicate that important nonlinear effects strongly stabilize the system. These numerical simulations also confirmed the prediction of a linear dependence of λ as a function of the detuning and its dependence on the perturbation amplitude. A great number of open problems subsists. Among them, let us mention those under present consideration for a planned work. A more detailed analysis of the different scaling laws appearing in the problem together with the comparison of the different time scales relevant for the system (see Ref. 13). The relation between the underlying geometrical structure and the observed change of behavior of the system also seems an important point to be enlightened.

ACKNOWLEDGMENTS

Stimulating and helpful discussions with D. Escande and M. Rasetti are gratefully acknowledged. One of us (M.P.) wishes to thank D. Ruelle for comments at the early stages of the present work. Computer simulations have been financially supported by the Istituto Nazionale di Fisica Nucleare and the Consiglio Nazionale delle Ricerche which are hereby warmly acknowledged. The Centre de Physique Théorique (CPT) is "Laboratoire Propre No. 7061 du Centre National de la Recherche Scientifique (CNRS). R. L. thanks the Osservatorio Astrofisico di Arcetri for the kind hospitality and financial aid. M. P. thanks the CPT-CNRS and the Faculté des Sciences, Université Marseille II for kind hospitality and financial aid.

APPENDIX

Let us briefly sketch how Eq. (7) is derived. Equation (3) can be trivially rewritten as

$$\begin{bmatrix}\dot{x}\\ \dot{p}\end{bmatrix}=\begin{bmatrix}p\\ x-\beta x^3\end{bmatrix}+\epsilon\begin{bmatrix}0\\ -\frac{\delta}{\epsilon}p+\frac{\gamma}{\epsilon}\cos(\omega t)-\frac{\beta\eta}{\epsilon}\cos(\Omega t)x^3\end{bmatrix}, \quad \text{(A1)}$$

which is in the form

$$\dot{\mathbf{x}}=\mathbf{f}_0(\mathbf{x})+\epsilon\mathbf{f}_1(\mathbf{x},t)\ , \quad \text{(A2)}$$

where $\dot{\mathbf{x}}=\mathbf{f}_0(\mathbf{x})$ is the integrable part derived from the Hamiltonian (4). The Melnikov distance, at first order in the smallness parameter ϵ, is[9]

$$\Delta(t_0)=-\int_{-\infty}^{\infty}dt(\mathbf{f}_0\times\mathbf{f}_1)_{\Gamma^{(0)}(t-t_0)}\ , \quad \text{(A3)}$$

and it is calculated along $\Gamma^{(0)}(\tau)$, the unperturbed homoclinic loop parametrically defined by Eq. (6).

---

*Permanent address: Osservatorio Astrofisico di Arcetri, Largo Enrico Fermi 5, 50125 Firenze, Italy.

[1]V. I. Arnold, *Les Méthodes Mathématiques de la Méchanique Classique* (MIR, Moscow, 1976).

[2]V. I. Arnold and A. Avez, *Ergodic Problems of Classical Mechanics* (Benjamin, New York, 1968).

[3]R. Abraham and J. E. Marsden, *Foundations of Mechanics* (Cummings, Reading, 1978).

[4]M. M. Postnikov, *The Variational Theory of Geodesics* (Dover, New York, 1983).

[5]H. T. Davis, *Introduction to Nonlinear Differential and Integral Equations* (Dover, New York, 1962).

[6]R. A. Mahaffey, Phys. Fluids **19**, 1387 (1976).

[7]M. Pettini *et al.*, Phys. Rev. A **38**, 344 (1988); M. N. Rosenbluth, R. Z. Sagdeev, J. B. Taylor, and G. M. Zaslavsky, Nucl. Fusion **6**, 297 (1966).

[8]See, for instance, A. Gerasimov, F. M. Izrailev, J. L. Tennyson, and A. B. Temnykh, in *Nonlinear Dynamics Aspects of Particle Accelerators*, Vol. 247 of *Lecture Notes in Physics*, edited by J. M. Jowett, M. Month, and S. Turner (Springer-Verlag, Berlin, 1986).

[9]J. Guckenheimer and P. J. Holmes, *Nonlinear Oscillations, Dynamical Systems and Bifurcation of Vector Fields* (Springer-Verlag, New York, 1983).

[10]V. K. Melnikov, Trans. Moscow Math. Soc. **12**, 1 (1963).

[11]V. I. Arnold, *Chapitres Supplémentaires de la Théorie des Equations Differentielles Ordinaires* (MIR, Moscow, 1980), Chap. 3.

[12]B. V. Chirikov, Phys. Rep. **52**, 263 (1979).

[13]P. Holmes, Philos. Trans. R. Soc. London Ser. A **292**, 419 (1979).

[14]F. T. Arecchi, R. Badii, and A. Politi, Phys. Rev. A **32**, 402 (1985).

[15]G. Benettin, L. Galgani, and J. M. Strelcyn, Phys. Rev. A **14**, 2338 (1976).